Contrib Mineral Petrol (2004) 147: 228–240
DOI 10.1007/s00410-004-0556-4

ORIGINAL PAPER

Stefanie Schwarz · Andreas Klügel
Cora Wohlgemuth-Ueberwasser

Melt extraction pathways and stagnation depths beneath the Madeira and Desertas rift zones (NE Atlantic) inferred from barometric studies

Received: 14 August 2003 / Accepted: 19 December 2003 / Published online: 17 February 2004

Abstract The Madeira and Desertas Islands (eastern North Atlantic) show well-developed rift zones which intersect near the eastern tip of Madeira (São Lourenço peninsula). We applied fluid inclusion barometry and clinopyroxene-melt thermobarometry to reconstruct levels of magma stagnation beneath the two adjacent rifts and to examine a possible genetic relationship during their evolution. Densities of CO_2-dominated fluid inclusions in basanitic to basaltic samples from São Lourenço yielded frequency maxima at pressures of 0.57–0.87 GPa (23–29 km depth) and 0.25–0.32 GPa (8–10 km), whereas basanites, basalts and xenoliths from the Desertas indicate 0.3–0.72 GPa (10–24 km) and 0.07–0.12 GPa (2–3 km). Clinopyroxene-melt thermobarometry applied to Ti-augite phenocryst rim and glass/groundmass compositions indicates pressures of 0.45–1.06 GPa (15–35 km; São Lourenço) and 0.53–0.89 GPa (17–28 km; Desertas Islands) which partly overlap with pressures indicated by fluid inclusions. We interpret our data to suggest a multi-stage magma ascent beneath the Madeira Archipelago: main fractionation occurs at multiple levels within the mantle (> 15 km depth) and is followed by temporary stagnation within the crust prior to eruption. Depths of crustal magma stagnation beneath São Lourenço and the Desertas differ significantly, and there is no evidence for a common shallow magma reservoir feeding both rift arms. We discuss two models to explain the relations between the two adjacent rift systems: Madeira and the Desertas may represent either a two-armed rift system or two volcanic centres with separate magma supply systems. For petrological and volcanological reasons, we favour the second model and suggest that Madeira and the Desertas root in distinct regions of melt extraction. Magma focusing into the Desertas system off the hotspot axis may result from lithospheric bending caused by the load of the Madeira and Porto Santo shields, combined with regional variations in melt production due to an irregularly shaped plume.

Electronic Supplementary Material Supplementary material is available for this article if you access the article at http://dx.doi.org/10.1007/s00410-004-0556-4. A link in the frame on the left on that page takes you directly to the supplementary material.

Editorial responsibility: J. Hoefs

S. Schwarz (✉) · A. Klügel · C. Wohlgemuth-Ueberwasser
Department of Geology, University of Bremen, Klagenfurter Straße, Geb. GEO, 28359 Bremen, Germany
E-mail: sschwarz@uni-bremen.de
Tel.: +49-421-2188974
Fax: +49-421-2189460

Introduction

Little is known about magma transport within the lithosphere slowly moving over a hotspot. Although studies of hotspot-related volcanic ocean islands such as Hawaii, the Canary Islands and Iceland have led to a better understanding of magma plumbing systems of ocean island volcanoes (Hawaii: e.g. Eaton and Murata 1960; Duffield et al. 1982; Clague 1987; Ryan 1988; Delaney et al. 1990; Tilling and Dvorak 1993; Canary Islands: e.g. Hansteen et al. 1998; Klügel et al. 2000; Iceland: e.g. Gudmundsson 1995), central questions remain. These include why different magma reservoirs form beneath the volcanoes, their depths, their evolution over time and their control on magma petrogenesis. Moreover, it is not clear how magma supply systems of adjacent volcanoes may be interconnected and which inferences can be made about melt pathways within the lithosphere.

The Madeira Archipelago is an ideal site to study the evolution of hotspot-related volcanoes and their rift zones in detail. The unique feature of the archipelago is the occurrence of two well-developed volcanic rift zones exposed by deep erosion: the E–W-trending Madeira rift zone and the NNW–SSE-oriented Desertas rift. They have been interpreted to represent a two-armed volcanic

rift system, with activity shifting between both arms (Geldmacher et al. 2000). The possible genetic relationship of the magma supply systems of the two rift arms is, however, still unknown.

Thermobarometry is a suitable approach to address this question. Former studies have shown that depths of magma storage can be estimated from densities of fluid inclusions trapped in phenocrysts and xenoliths (Roedder 1965, 1983; De Vivo et al. 1988; Belkin and De Vivo 1993; Szábo and Bodnar 1996; Hansteen et al. 1998; Andersen and Neumann 2001). In addition, pressure and temperature can be derived from the compositions of glass and coexisting clinopyroxene phenocryst rims to infer depths of magma reservoirs (Putirka et al. 1996).

In this paper, we present fluid inclusion and clinopyroxene-melt thermobarometric data from the Desertas Islands and São Lourenço, the easternmost tip of Madeira located near the projected junction between the two rift arms. Our geobarometric data, combined with geochronological data on the evolution of the islands, provide a first model of magma storage beneath the two rifts. We compare our results with current models of magma transport and storage beneath two-armed rift systems such as Kilauea, and discuss if and how the Madeira and Desertas rifts may have been interconnected. Finally, we show what constraints can be placed on the distribution of volcanism of the Madeira/Desertas complex.

Geological setting

The Madeira Archipelago is located in the eastern North Atlantic, 700 km from the north-western coast of Africa. The archipelago consists of five islands: Madeira, Porto Santo and the three Desertas Islands (from N to S: Ilhéu Chão, Deserta Grande, Ilhéu Bugio; Fig. 1). The island of Madeira is interpreted as the present locus of the Madeira hotspot which can be traced back to 70 Ma (Geldmacher et al. 2000). The main island rises from about 4,000-m water depth to an elevation of 1,896 m above sea level, and the Desertas to an elevation of 480 m. The underlying oceanic crust is about 140 Ma old (Pitman and Talwani 1972).

Madeira and the Desertas Islands are interpreted to represent a single volcanic complex, with a two-armed rift system consisting of the E–W-oriented Madeira rift arm and the NNW–SSE-oriented Desertas rift arm (Geldmacher et al. 2000). Their rift axes intersect at an angle of ~110° near Ponta de São Lorenço, the easternmost tip of Madeira (Fig. 1). The Madeira-Desertas volcanic system is characterised by a shield stage and a post-erosional stage (Geldmacher et al. 2000). The shield stage can be divided into (1) the Early Madeira rift phase (EMRP, >4.6–3.9 Ma), comprising the submarine basement and the oldest subaerial rocks of Madeira, (2) the Desertas rift phase (DRP, 3.6–3.2 Ma), with a shift

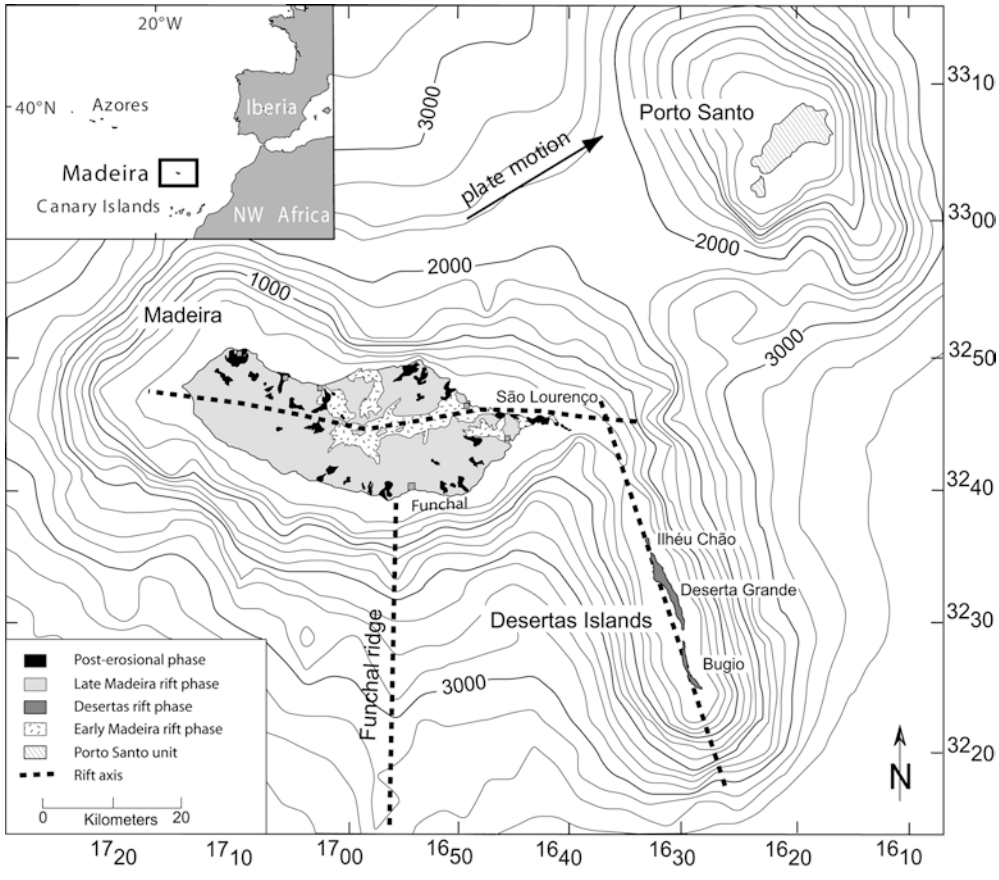

Fig. 1 Bathymetric and geological map of the Madeira Archipelago. Source of bathymetry: TOPEX (Smith and Sandwell 1997); geology modified after Geldmacher et al. (2000). Near São Lourenço, the axes of the Madeira and Desertas rift zones intersect each other at an angle of 110°. The NS-trending submarine ridge south of Funchal is also interpreted as a volcanic rift zone and presumably represents the location of most recent volcanic activity

of subaerial volcanic activity from the Madeira rift to the Desertas rift arm, and (3) the Late Madeira rift phase (LMRP, 3.0–0.7 Ma), during which the activity switched back to Madeira along the E–W-trending rift system. During the post-erosional stage (PE, <0.7 Ma), cinder cones, tephra layers and intracanyon flows were deposited after a period of inactivity and erosion. New $^{40}Ar/^{39}Ar$ age determinations (van den Bogaard, unpublished data) show that the oldest subaerial rocks on Madeira are exposed on São Lourenço and that the stratigraphic sequence of the peninsula covers the complete Madeira shield stage with ages of 5.1–4.0 Ma (EMRP) and 2.6–0.97 Ma (LMRP). Furthermore, the new data indicate that subaerial volcanism on the Desertas extended from at least 5.07 to 2.7 Ma, and thus partly overlaps with the Early and Late Madeira rift phases.

Another rift arm of Madeira is located to the south of Funchal (Fig. 1) and forms a 50-km-long, submarine ridge with at least a dozen volcanic cones which occur clustered at the southern tip. This structure, hereafter referred to as the Funchal ridge, was discovered, mapped and sampled during cruise M51/1 of the German research vessel Meteor (Hoernle et al. 2001). The freshness of most samples suggests that this rift arm may still be active.

Rock types

Madeira and the Desertas Islands are characterised by alkaline rocks ranging from picrites and basanites to benmoreites (Fig. 2). The main phenocryst phases of alkali basalts and basanites from the Desertas Islands and São Lorenço are olivine and clinopyroxene (Ti-rich augite). Some basalts and hawaiites additionally contain plagioclase phenocrysts. Despite similar whole-rock geochemistry, significant and systematic petrographic differences between São Lorenço and the Desertas Islands can be observed (see Table 1). Olivine and especially clinopyroxene megacrysts (>1 cm in size) occur commonly on the Desertas Islands but only locally on São Lorenço. Amphibole megacrysts (up to 4-cm diameter) occur exclusively on the Desertas Islands. Basalts with olivine as the only phenocryst phase are abundant on São Lourenço, whereas Desertas basalts usually contain olivine plus clinopyroxene phenocrysts. Fluid inclusions are far more abundant in phenocrysts of Desertas basalts than in those from São Lorenço. These observations suggest distinctive magma chamber processes, magma ascent rates and/or stagnation levels.

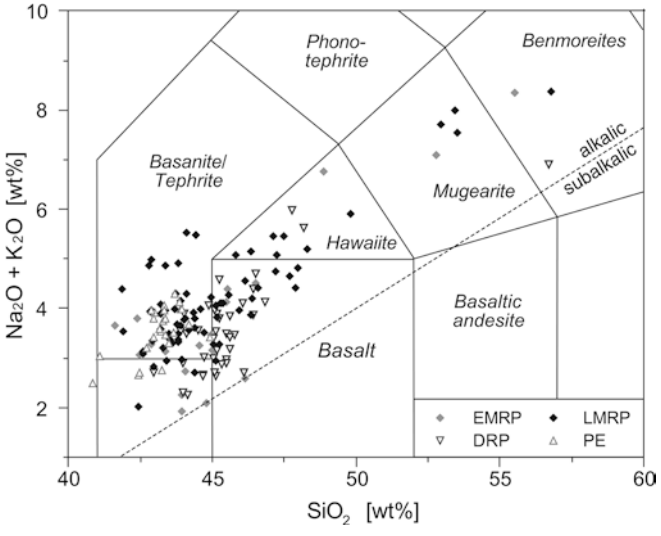

Fig. 2 TAS diagram of basaltic samples from the rift phases of the Madeira/Desertas volcanic complex (Geldmacher and Hoernle 2000), using the field boundaries of Le Maitre et al. (1989). Volcanic rocks are subdivided into alkalic and subalkalic after McDonald (1968). *EMRP* Early Madeira rift phase, *DRP* Desertas rift phase, *LMRP* Late Madeira rift phase, *PE* post-erosional phase on Madeira

Analytical methods

Geobarometric data were obtained by microthermometry of fluid inclusions and by mineral-melt equilibria. Fluid inclusions were observed in 100-μm, doubly polished plates from lavas, dikes and xenoliths from Deserta Grande and Bugio (Desertas Islands), São Lourenço and the Funchal ridge. Microthermometric measurements were carried out on a Linkam THMSG 600 heating-cooling stage calibrated with SYNFLINC synthetic fluid inclusion standards at −56.6 (CO_2) and 0 °C (H_2O). Melting and homogenisation temperatures are reproducible to better than ±0.2 °C. Inclusion densities were derived from Angus et al. (1976), and isochores were calculated using the computer program Flincor (Brown 1989), utilizing the Kerrick and Jacobs (1981) equation of state for the CO_2–H_2O system. In order to determine the possible presence of components other than CO_2, Raman microspectroscopy of two representative samples was carried out at the Institute of Geoscience, University of Leoben.

Mineral and glass analyses were performed on JEOL JXA 8900 electron microprobes (universities of Göttingen, Frankfurt and Kiel) operated at an acceleration voltage of 15 kV. Glasses were analysed with a beam current of 8 nA and a defocussed beam of 10 μm, minerals with 20 nA and a focussed beam. To determine average compositions, at least 15 points per glass sample and four points per clinopyroxene were measured.

Fluid inclusion barometry

All samples studied are porphyritic with 10–15% olivine and clinopyroxene phenocrysts, some containing plagioclase as additional phenocryst phase. Most Bugio basalts are ankaramites with 40–50% phenocrysts up to 1 cm in size. In addition, fluid inclusions in two xenoliths of spinel wehrlite (DES4) and spinel dunite (DGR132) from Deserta Grande and in a harzburgite xenolith from the southern tip of the Funchal ridge were analysed. Petrographic descriptions of xenoliths are given in the Appendix.

Table 1 Lithological and petrographic differences between Desertas and São Lorenço volcanics

		Desertas Islands	São Lourenço EMRP	LMRP
Field observations				
Ankaramites		Abundant as lava flows and tuffs	Rare	Very rare
Phenocrysts >4 mm		Abundant, especially cpx crystals up to 2-cm diameter	Rare, max. -cm diameter	Very rare
Xenoliths		Some peridotites and few gabbros	None	None
Petrographic observations				
Phenocrysts	Ol and cpx	Nearly always ol plus cpx (~90% of samples)	Commonly ol plus cpx (~75% of samples)	Only ol in ~55% of samples
	Plag	Tabular habit Single crystals	Elongated habit Often glomerocrysts	Very rare
	Amph	Megacrysts up to 4-cm diameter in some lavas and pyroclastics	None	None
Fluid inclusions in phenocrysts		Abundant	Very rare	Rare

Occurrence of fluid inclusions

Several generations of CO_2-dominated fluid inclusions occur abundantly in olivine and clinopyroxene phenocrysts and in the xenoliths. They can be divided into (1) primary inclusions occurring singly or in groups which do not form trails, and (2) secondary or texturally late inclusions forming trails reaching, and sometimes crossing, grain boundaries. Some inclusions which show textural evidence of partial decrepitation with measurable fluid phases were not incorporated. Common inclusion sizes are 3 to 15 μm, seldom >20 μm. In general, fluid inclusions are far more abundant in phenocrysts of samples from the Desertas Islands than from São Lourenço. In the xenoliths, secondary fluid inclusions are the main inclusion type and are common in olivine, but relatively rare in clinopyroxene.

Microthermometry of fluid inclusions

Composition of fluid inclusions

Upon rapid cooling, all fluid inclusions froze to aggregates between −70 and −100 °C of solid CO_2; further cooling to about −190 °C produced no visible phase changes. Upon heating of the inclusions from about −190 °C, the following phase transitions were observed: (1) initial and final melting of CO_2 (Tm) between −57.4 and −56.4 °C, and (2) final homogenisation of liquid and vapour (L + V) into liquid (Th_L) or into vapour (Th_V) at less than 31.1 °C. In many cases, phase transitions of inclusions homogenising into vapour could not be accurately determined due to optical constraints. Therefore, Th_V data do not reveal distinct statistical maxima but, nevertheless, they have to be considered as significant.

Few inclusions show Tm below the triple point for pure CO_2 (−56.6 °C), which most likely results from thermal gradients in the heating-cooling stage. Raman analysis of some of these inclusions revealed no fluid components other than $CO_2$and traces of CO. There is no evidence for the presence of H_2O, although H_2O is expected as a component in fluids exsolved from mafic melts (Dixon et al. 1997). This indicates that diffusive hydrogen loss from fluid inclusions may have occurred at high temperatures (Bakker and Jansen 1991), changing original fluid inclusion compositions. Another feasible process to remove H_2O from the inclusion fluid are hydration reactions between the fluid and the host mineral forming secondary minerals such as amphiboles, sheet silicates or carbonates (Andersen et al. 1984; Andersen and Neumann 2001; Frezotti et al. 2002). We did not observe any sign of secondary products, although this may be related to small inclusion diameters (mostly <10 μm).

By assuming that the fluid phase coexisting with mafic melt had an $XH_2O = H_2O/(CO_2 + H_2O)$ of 0.1, which is an upper limit for basanitic melts at 1,000 MPa (Dixon et al. 1997; Sachs and Hansteen 2000), all calculated inclusion densities would increase by 4.5%. Because of possible error introduced by such an assumption, we present original rather than corrected density data throughout this study, calculated for pure CO_2, and consider the possible error in the discussion.

Homogenisation temperatures and inclusion densities

The measured homogenisation temperatures of all inclusions and their resulting densities are presented in Figs. 3 and 4. Inclusion densities show distinctive histogram maxima (intervals) in their frequency distribution. For convenience, we subsequently define the limits of each interval such as to comprise 90% of the respective data points.

Basalts and xenoliths from Deserta Grande Both primary and secondary fluid inclusions homogenised into liquid between 12.6 and 30.3 °C in olivine and at 14.8 to 27.8 °C in clinopyroxene. Some measured inclusions in olivine phenocrysts homogenised into vapour at 22 to

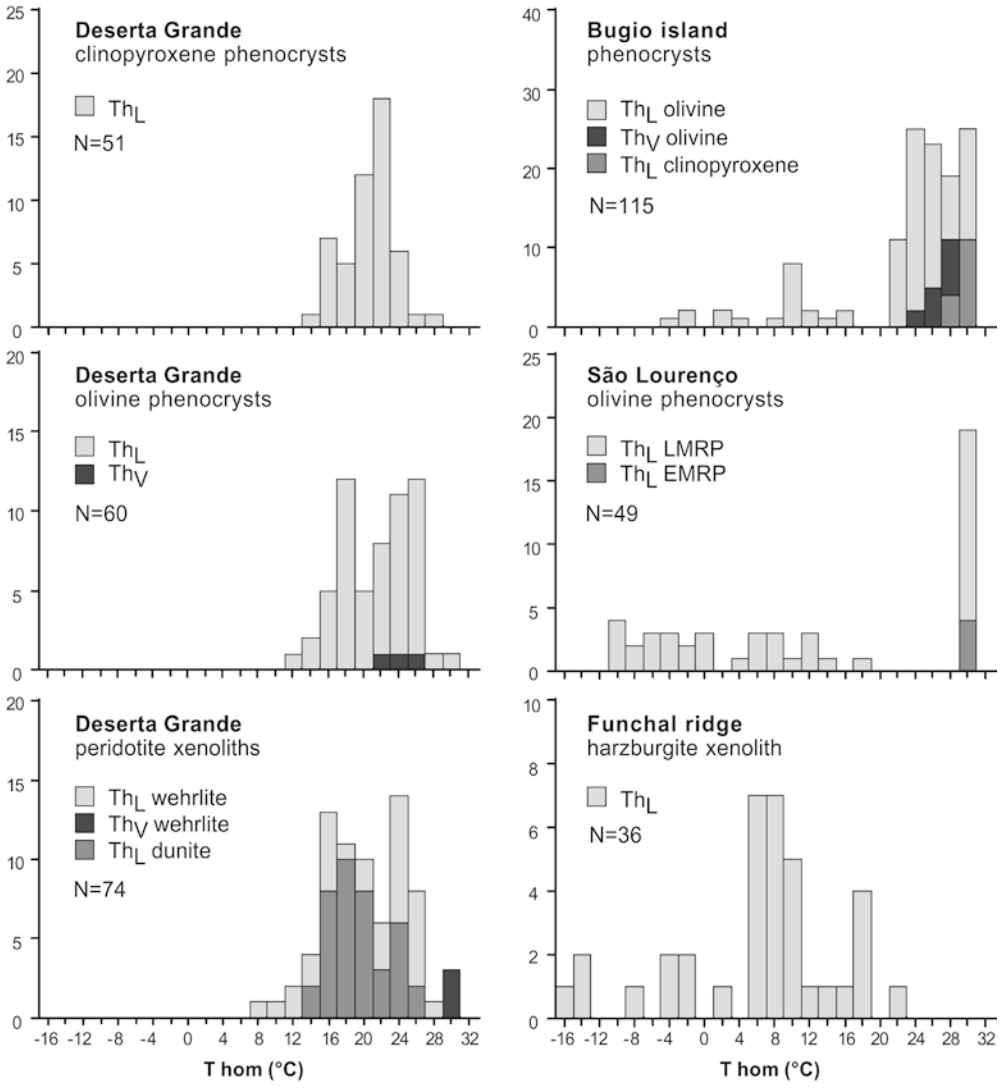

Fig. 3 Distribution of homogenisation temperatures of CO_2-dominated fluid inclusions in phenocrysts of basaltic rocks and xenoliths from the Desertas Islands and São Lorenço. Th_L homogenised into liquid, Th_V homogenised into vapour

25.3 °C (Th_V). These values correspond to densities ranging from 0.22 to 0.83 g cm^{-3} with two maximum intervals: (1) between 0.22 and 0.24 g cm^{-3} and (2) between 0.7 and 0.82 g cm^{-3}. Inclusions in olivine of peridotite xenoliths showed Th_L between 7.5 and 27.9 °C, and some inclusions in wehrlite olivine homogenised at $Th_V \sim 29$ °C. Resulting density maxima occur at 0.7 to 0.83 g cm^{-3}, overlapping with those of inclusions in phenocrysts, and at 0.31 to 0.32 g cm^{-3}.

Basalts from Bugio Almost all fluid inclusions were observed in olivine phenocrysts, with Th_L ranging from −4.3 to 30.9 °C. Homogenisation temperatures < 15 °C occur exclusively in texturally early fluid inclusions. Some inclusions show vapour homogenisation at 24.1 to 28.2 °C. Inclusions in clinopyroxene homogenised into liquid at 28.4 to 29.8 °C. These Th data give densities ranging from 0.23 to 0.95 g cm^{-3} with three frequency maxima: (1) 0.23 to 0.29 g cm^{-3}, (2) 0.6 to 0.75 g cm^{-3} and (3) 0.83 to 0.93 g cm^{-3}. In summary, the shallow and intermediate density maxima overlap with those from Deserta Grande, but a third higher-density range can additionally be observed.

Basalts from São Lourenço Primary as well as secondary inclusions were observed in olivine phenocrysts in one EMRP sample (SL106) and in three LMRP samples. In general, the inclusions homogenised into liquid at temperatures between −10 and 30.4 °C. Compared with samples from the Desertas Islands, homogenisation temperatures are more dispersed and tend to lower values. No fluid inclusions homogenising into vapour were found. Fluid inclusions in sample SL106 give densities of 0.60 g cm^{-3}. For the LMRP samples, resulting density maxima occur at (1) 0.56 to 0.60 g cm^{-3} and (2) 0.84 to 0.99 g cm^{-3}.

Harzburgite xenolith from the Funchal ridge Primary as well as texturally late fluid inclusions were observed in

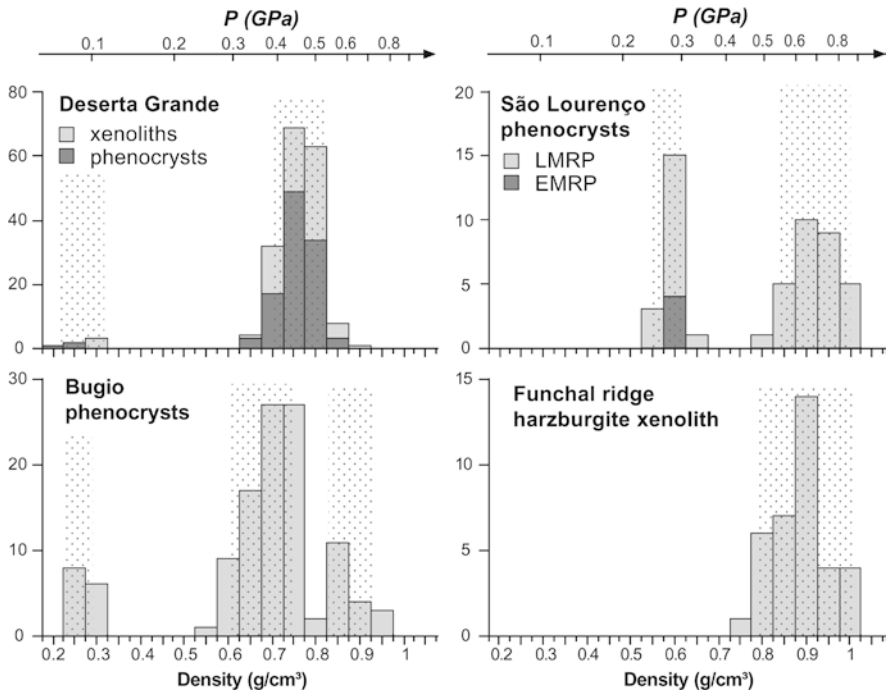

Fig. 4 Density distribution of CO_2-dominated fluid inclusions in basalts and xenoliths from the Desertas Islands and São Lorenço. Densities were derived from Angus et al. (1976). Pressures were calculated for model temperatures of 1,150 °C and pure CO_2, using the Kerrick and Jacobs (1981) equation of state. *Dotted areas* symbolise density intervals comprising 90% of the respective data points

olivine porphyroclasts. All homogenised into liquid between −15.1 and 22.5 °C, comprising the lowest homogenisation temperatures of this study. Resulting densities range from 0.74 to 1.01 g cm^{-3}, with a maximum between 0.78 and 1.01 g cm^{-3} overlapping with the high density ranges of the Desertas Islands and São Lourenço.

Pressures of inclusion formation

Density data of CO_2-dominated fluid inclusions can provide constraints on the pressures at which they were entrapped during crystal growth or crack healing or at which they re-equilibrated (Roedder and Bodnar 1980; Roedder 1984). Pressures of inclusion formation or re-equilibration corresponding to calculated densities were derived assuming a model temperature of 1,150 °C as based on clinopyroxene-melt thermobarometry (see below). Since isochores of CO_2 inclusions have moderately positive slopes (Fig. 6), variations in model temperature have only little effect on calculated pressures.

If one assumed a constant H_2O fraction of 10% rather than pure CO_2 for all inclusions, different isochores would result (Kerrick and Jacobs 1981). For a density range between 0.2 and 1.05 g cm^{-3} for pure CO_2 inclusions, as observed in the present study (Fig. 4), the corresponding pressures would increase from 0.063–1.01 (pure CO_2) to 0.07–1.28 GPa ($X_{H2O} = 10\%$), i.e. by 11 to 26%. These values may be considered as an upper limit of systematic error.

Due to decrease of inclusion densities by diffusive loss of H_2O as well as re-equilibration of fluid inclusions during magma ascent, the following estimates represent *minimum* pressures.

Desertas Islands

Densities indicated by fluid inclusions in phenocrysts from Desertas Grande overlap perfectly with those in xenoliths and yield two intervals corresponding to the following pressures: (1) 0.07 to 0.12 GPa, and (2) 0.4 to 0.53 GPa. Inclusion densities from Bugio samples largely overlap with these ranges (Fig. 4). However, three density intervals can be distinguished whose corresponding pressure limits slightly differ from those of Deserta Grande: (1) 0.075–0.1 GPa, (2) 0.29–0.44 GPa, and (3) 0.55–0.71 GPa.

São Lourenço

EMRP samples indicated pressures of 0.29 GPa, and fluid inclusion data of LMRP samples yield two density maxima corresponding to the following pressures: (1) 0.26 to 0.29 GPa and (2) 0.57 to 0.85 GPa. In contrast to the Desertas Islands, no shallow pressure range around 0.1 GPa could be identified, and no fluid inclusions yielded pressures between 0.32 and 0.49 GPa. The higher pressure range of São Lourenço partly overlaps with the highest pressure range indicated by fluid inclusions in samples from Bugio (Desertas), but tends to higher values.

Funchal ridge

Fluid inclusion densities from Funchal ridge samples yield pressures between 0.48 and 0.9 GPa, overlapping

with data from Desertas Islands and São Lourenço but extending towards higher pressures.

Clinopyroxene-melt thermobarometry

Mineral-melt equilibration pressure (P) and temperature (T) were calculated with the thermobarometer of Putirka et al. (1996) which is based on the exchange of jadeite/diopside/hedenbergite components between clinopyroxene and melt.

Sample description and preparation

Investigated lapilli samples from São Lourenço (SL163, LMRP), Deserta Grande (DGR101, DGR123) and Bugio (DBU101) have glassy to tachylitic groundmass with plagioclase, olivine and augite micro-phenocrysts (up to 300 μm, olivine up to 1 mm). Only sample DBU101 has clinopyroxene and plagioclase phenocrysts up to 4 mm. A submarine basalt (M51/1-447DR-1) from the southern tip of the Desertas ridge was investigated and has a tachylitic matrix with plagioclase, olivine and clinopyroxene phenocrysts and locally some fresh glass at the rim.

Since fresh glassy material was rare, some porphyritic samples were chosen for groundmass separation. These samples have a fresh matrix of plagioclase, clinopyroxene, olivine and Fe–Ti oxides in different ratios, and contain euhedral, optically zoned clinopyroxene and olivine phenocrysts. More differentiated samples (e.g. SL151) additionally contain elongated plagioclase phenocrysts. Separated matrix was powdered, fused on an Ir filament and quenched under air at the Institute of Mineralogy (University of Frankfurt).

Data selection

Pressure and temperature data are based on EMP analyses of coexisting augite rim and glass compositions. EMP measurements on sector-zoned clinopyroxenes were generally avoided. Possible equilibrium between clinopyroxenes and melt was tested following the empirical relation of Duke (1976):

$$\log(Fe_{tot}/Mg)_{cpx} = -0.564 + 0.755 * \log(Fe_{tot}/Mg)_{liq}$$

If the deviation between measured and predicted Fe/Mg ratio was significant for several analyses within a single clinopyroxene, the data were rejected. In case of a systematic deviation for all clinopyroxenes within a common sample, the data were incorporated. Such systematic deviations could be ascribed to differing redox potentials and Fe^{2+}/Fe^{3+} ratios which were not considered by Duke (1976).

According to Putirka et al. (1996), the mean prediction errors of the thermobarometer are ±30 K and ±140 MPa. As an independent consistency test of the data, calculated temperatures were compared to those of thermometers based on olivine + liquid equilibria (Roeder and Emslie 1970; Ford et al. 1983; Putirka 1997).

PT-calculations

Desertas Islands

Most samples from the Desertas Islands indicate pressures between 0.57 and 0.82 GPa and temperatures ranging from 1,140 to 1,180 °C (Table 2, Fig. 5). Ol-melt thermometers after Roeder and Emslie (1970), Putirka (1997) and Ford et al. (1983) predict equilibrium temperatures between 1,170 and 1,175 °C which largely agree with the cpx-melt data. Although data obtained by mineral-melt barometry overlap with the highest pressure range indicated by fluid inclusions (Fig. 6b), they generally tend to higher pressures. This difference can be related to re-equilibration of fluid inclusions during magma ascent as well as decrease of inclusion densities by diffusive loss of H_2O.

Pressure predictions of sample K8 from Bugio are exceptional since they scatter over a wide range between 0.13 and 0.89 GPa (Table 2). The values largely overlap with the pressure ranges indicated by fluid inclusions within the prediction error of the clinopyroxene-melt barometer (Fig. 6).

São Lourenço

Mineral-melt thermobarometry applied to EMRP samples yield pressures between 0.45 and 1.06 GPa (Fig. 5). The data can be divided into two PT intervals: (1) from 0.45 to 0.68 GPa and 1,160 to 1,190 °C, and (2) from 0.7 to 1.06 GPa and 1,180 to 1,235 °C (Figs. 5, 6a). Both P intervals overlap with the highest pressure range for fluid inclusions in LMRP samples from São Lourenço (0.56–0.83 GPa; Fig. 6a). Deviations of pressure estimates below the range for fluid inclusions are within the prediction error of the barometer (±0.14 GPa). Compared to data from the Desertas Islands, the range of pressure estimates for São Lourenço tends to higher values, in accordance with results from the fluid inclusion barometry.

The LMRP lapilli sample (SL163) yields temperatures of 1,150–1,160 °C which are in accordance with crystallisation temperatures of peridotite xenoliths from NW and SE Madeira (1,150–1,300 °C; Munha et al. 1990). Calculated pressures range from 0.56 to 0.64 GPa and overlap clearly with the lower P interval indicated by EMRP samples and, additionally, with the highest pressure range for fluid inclusions in LMRP samples (Fig. 6c).

Discussion

Depths of magma fractionation and stagnation

Our thermobarometric data provide the base for a first model of magma plumbing systems beneath the

Table 2 Results of PT calculations after Putirka et al. (1996)

São Lourenço						Desertas Islands							
Sample#	SL2[a]	SL106[a]	SL122[a]	SL150[a]	SL151[a]	SL152[a]	SL163[b]	DGR101	DGR123	DGR29	DBU101	M51/1-447DR-1	K8
No. of cpx	6	8	9	8	4	9	6	5	6	6	5	5	6
P range (GPa)	0.5–0.63	0.45–0.68, 1.02–1.06	0.47–0.57, 0.7–0.95	0.75–0.91	0.58, 0.78–1.01	0.79–1.03	0.56–0.64	0.57–0.69	0.57–0.66	0.67–0.82	0.6–0.73	0.58–0.68	0.13–0.15, 0.37, 0.53–0.56, 0.89
T range (°C)	1,160–1,170	1,170–1,190, 1,220	1,184–1,190, 1,201–1,219	1,195–1,210	1,167, 1,182–1,199	1,215–1,235	1,150–1,160	1,165–1,175	1,145–1,150	1,175–1,185	1,150–1,160	1,150–1,160	1,120, 1,137, 1,150, 1,179
P mean of range (GPa)	0.55	0.57, 1.04	0.51, 0.85	0.85	0.58, 0.88	0.95	0.61	0.63	0.61	0.76	0.68	0.65	
T mean of range (°C)	1,165	1,180,1,220	1,186,1,214	1,205	1,167,1,190	1,227	1,154	1,147		1,180	1,153	1,153	
Rock type	Basaltic lava flow	Basaltic dike	Basaltic dike	Basaltic dike	Basanitic dike	Basaltic dike	Lapilli	Lapilli	Lapilli	Basanite flow	Lapilli	Basanite	Beach boulder (basalt)

[a]Early Madeira rift phase
[b]Late Madeira rift phase

Fig. 5a, b Crystallisation pressures of clinopyroxene phenocrysts in basaltic rocks from **a** the Desertas Islands and **b** São Lorenço, obtained by clinopyroxene-melt barometry after Putirka et al. (1996). Each pressure value represents the conditions of crystallisation for a single clinopyroxene phenocryst

Madeira/Desertas volcanic complex. We interpret the pressure calculations derived from mineral-melt barometry to reflect major levels of crystal fractionation. The pressure data obtained by fluid inclusion barometry were interpreted to imply magma stagnation, degassing and crystal fractionation at a corresponding range of depths. Since inclusion densities may rapidly re-equilibrate during ascent, they additionally indicate depths of temporary magma stagnation at shallower levels.

São Lourenço—Early Madeira rift phase

During the EMRP, major levels of magma fractionation beneath São Lourenço were located at 15–35 km depth, as documented by clinopyroxene-melt barometry (Fig. 6a). Further magma stagnation at about 9 km depth is manifested by few fluid inclusions, but not by clinopyroxene-melt barometry. This observation suggests that magmas stagnated temporarily in the lower oceanic crust.

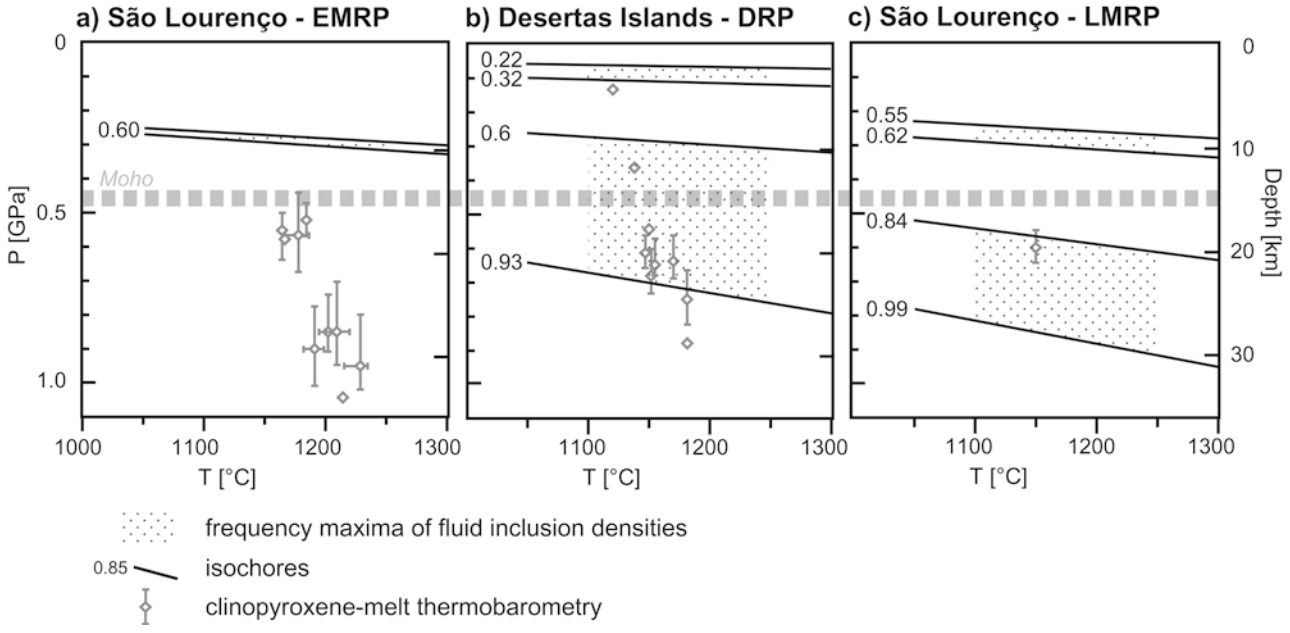

Fig. 6a–c PT diagram summarising fluid inclusion and mineral-melt barometry data applied to basaltic rocks from **a** São Lourenço (*EMRP* Early Madeira rift phase),**b** the Desertas Islands (*DRP*Desertas rift phase) and **c** São Lorenço (*LMRP* Late Madeira rift phase). *Dotted areas* Frequency intervals of fluid inclusion density (see Fig. 4), *shaded symbols* ranges of PT conditions of clinopyroxene fractionation, *quadrangles*mean values of the respective ranges (see Table 2)

Desertas Islands—Desertas rift phase

Clinopyroxene-melt barometry indicates major crystal fractionation of Desertas lavas at 17–28 km depth (Fig. 6b). This range overlaps well with fluid inclusion data from Bugio which yield a density maximum corresponding to pressures between 0.55 and 0.72 GPa (18–23 km depth, Fig. 4). Further magma stagnation, degassing and crystallisation of mafic magmas at 9–17 km depth is manifested by fluid inclusion data from Deserta Grande as well as Bugio (Fig. 6b), and by clinopyroxene-melt barometry (sample K8, Table 2). Fluid inclusions in phenocrysts and xenoliths from Deserta Grande yield a significant frequency maximum at pressures between 0.39 and 0.55 GPa (Fig. 4), corresponding to 12–16 km depth. This range may coincide with the Moho which we suppose to be located at 14–15 km depth, by analogy to the western Canary Islands (Banda et al. 1981) showing a similar age of the underlying oceanic crust (ca. 160 Ma, Roeser 1982). The data may thus reflect a main stagnation and fractionation level near the Moho, possibly a crystal mush zone. This situation is comparable to the Canary Islands where fluid inclusions indicate that primitive melts and their xenoliths may reside at Moho or lower crustal depths prior to eruption (Hansteen et al. 1998).

Finally, both fluid inclusions and mineral-melt barometry indicate a further level between 2 and 4 km depth (Fig. 6b), which demonstrates resetting of fluid inclusions and additional clinopyroxene fractionation at shallower depths during temporary magma stagnation. This stagnation level coincides with a level of neutral buoyancy inferred for the Kilauea volcano, Hawaii (Ryan 1988), and could reflect shallow rift pathways in the upper crust near the base of the volcanic edifice (Fig. 7a).

São Lourenço—Late Madeira rift phase

Main fractionation levels of lavas erupted during the LMRP are located at 18–28 km depth as indicated by fluid inclusion barometry as well as clinopyroxene-melt barometry (Figs. 6c, 7). This range overlaps with fractionation depths during the EMRP and with fractionation levels indicated by Desertas samples.

In contrast, a geobarometric study applied to ultramafic cumulate xenoliths in LMRP units from NW and SE Madeira infers pressures of phenocryst accumulation between 1.2 and 1.5 GPa corresponding to magma reservoirs at 39–48 km depth (Munha et al. 1990). Since our pressure calculations reflect the last equilibration conditions of clinopyroxene prior to eruption and do not preclude deeper magma reservoirs, we believe that the combined data indicate crystal fractionation occurring over a wide depth range.

As is the case for EMRP samples, another shallower pressure range at 0.26 and 0.32 GPa is indicated only by fluid inclusions (Fig. 6c) and suggests temporary magma stagnation at 8–10 km depth in the lower oceanic crust prior to eruption (Fig. 7a).

Funchal ridge

Fluid inclusion densities presented from the southern tip of the Funchal ridge indicate major fractionation between 16 and 28 km depth. Magma stagnation within the upper crust is not indicated by our dataset. Since the

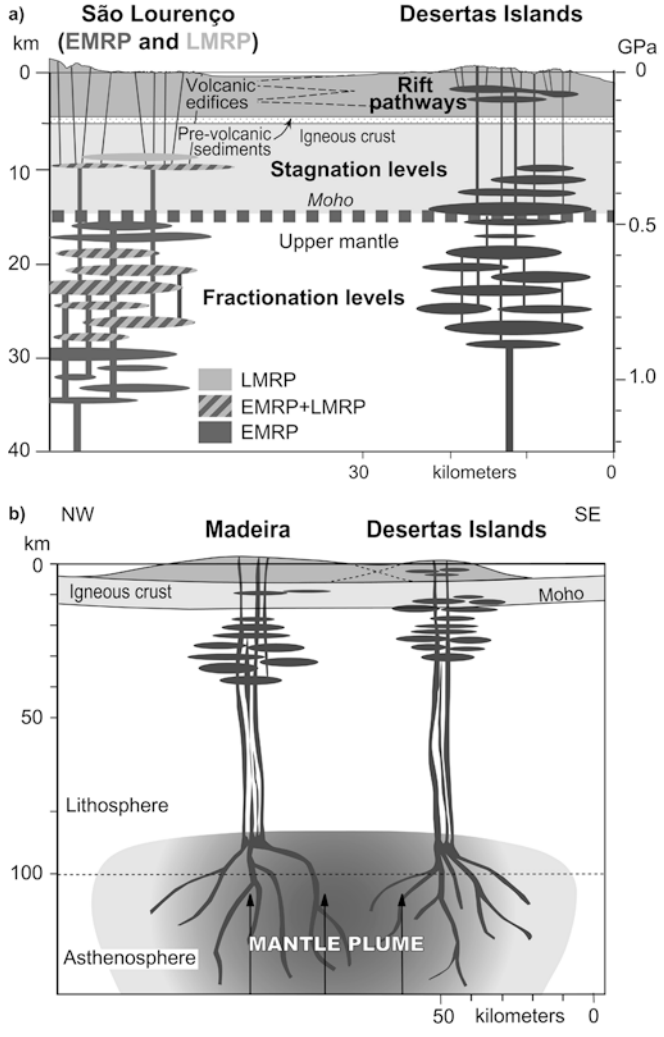

Fig. 7a Section through the oceanic crust and the uppermost mantle illustrating our model of magma transport and storage systems beneath São Lorenço and the Desertas Islands. **b** Sketch of inferred melt extraction pathways. Madeira and the Desertas are interpreted to represent two volcanoes which root in distinct regions of melt extraction within the ascending mantle plume

Funchal ridge is supposed to be the youngest magmatic system of the Madeira Archipelago (Hoernle et al. 2001), shallow stagnation levels may not have developed yet.

Two-armed rift system or separate volcanic systems?

Our data indicate significant differences as well as some similarities between the magma plumbing systems and inferred stagnation levels beneath São Lorenço and the Desertas Islands (Fig. 7). The observations can be explained by two end-member models: (1) the island of Madeira and the Desertas ridge represent two rift arms of a single volcanic system with an interconnection near São Lourenço (Geldmacher et al. 2000), or (2) they represent two separate volcanic systems with independent magma plumbing systems.

Model 1: two-armed rift system

Multiple-armed rift systems are a common feature of oceanic island volcanoes such as Kilauea/Hawaii (Walker 1999) or Tenerife/Canary Islands (Carracedo 1994). Typically, these systems are characterised by a central volcano from which two or three rift arms extend. In the case of Kilauea, the central summit is underlain by a shallow magma reservoir at 2–4 km depth (Ryan 1988) which feeds two rift arms by lateral magma injection mostly along dikes. The following observations point to an interconnection of the Madeira and the Desertas rifts in terms of a two-armed system analogous to Kilauea:

1. Madeira and the Desertas ridge intersect each other near São Lourenço and appear to form a continuous volcanic edifice (Fig. 1), suggesting that both rift arms extend from a centre near the eastern tip of Madeira.
2. The gap in volcanic activity on Madeira during the Desertas rift phase may indicate a close link between the respective magma supply systems, such as an interconnection of magma reservoirs.
3. Mineral-melt barometry as well as fluid inclusion barometry of samples from the Madeira and Desertas rift phases indicate overlapping fractionation levels at 15–28 km depth (Figs. 6, 7a). This may suggest a common magma reservoir and/or lateral magma transport to the rift zones at these depths, possibly along the mantle–oceanic crust boundary where density changes and subhorizontal layering could facilitate such a scenario.
4. Major element, trace element and radiogenic isotope characteristics of shield-stage volcanics from Madeira and the Desertas are broadly similar and show a continuous evolution over time (Geldmacher and Hoernle 2000), which suggests a common magma source for both systems.

Model 2: separate volcanic systems

The alternative model considers Madeira and the Desertas as two discrete, overlapping volcanoes with separate magma supply systems, a situation analogous to, e.g. the adjacent Kilauea and Loihi edifices. The following observations and considerations argue in favour of this hypothesis:

1. There is no petrological or field evidence for a shallow magma reservoir near São Lourenço, arguing against lateral magma transport from a central reservoir into the Madeira and Desertas rift arms. In addition, the inferred depths of shallow magma stagnation beneath São Lourenço during both the Early and Late Madeira rift phases are significantly below those of the Desertas rift phase (Fig. 6). There is thus no progressive evolution of a crustal storage system towards shallower depths as proposed for Hawaiian volcanoes (Clague 1987), which is suggestive of two separate magma plumbing systems.

2. If the magma supply systems of Madeira and the Desertas had been interconnected, lateral magma transport over tens of kilometres must have taken place in the uppermost mantle or near the Moho where fractionation levels overlap (Fig. 7). Lateral transport along dikes is possible only where an appropriate stress field exists, e.g. within a volcanic edifice (Dieterich 1988). Alternatively, if horizontal compressive stresses are higher than the vertical stress, horizontal intrusions may form (Gudmundsson 1995). Both scenarios, however, seem unlikely to provoke lateral magma transport over tens of kilometres in the uppermost mantle beneath Madeira.
3. There are systematic lithological differences between the São Lourenço and Desertas samples (Table 1). Moreover, fluid inclusions in São Lourenço samples are far less abundant than in Desertas rocks, indicating less fluid entrapment during crystal growth or crack healing. This implies either faster magma ascent from the fractionation levels to the surface, less degassing during fractionation, slower crystal growth, or different volatile contents of the parental magmas. These differences are best explained by distinctive magma transport systems beneath São Lourenço and the Desertas.
4. The present morphology is characterized by maximum elevations in the central parts of Madeira and the Desertas and a depression, rather than a rise, near the intersection of both rift axes (Fig. 1). Moreover, units of the EMRP occur up to 1,300 m above sea level in central parts of Madeira (Geldmacher et al. 2000), but only up to 175 m on São Lourenço. Such morphology and stratigraphy are hard to reconcile with a two-armed rift system emerging from a central volcano near São Lourenço.

Inferences on volcano distribution

After considering all arguments discussed above, we favour the model of two separate volcanoes with distinct magma plumbing systems (Fig. 7). As a consequence, the Madeira and Desertas volcanoes should root in distinct regions of melt extraction within the ascending mantle plume (Fig. 7b). The question arises, then, why the spatial and temporal succession of volcanic activity of the Madeira-Desertas complex is not in accordance with that expected from the hotspot track (Fig. 1). We propose the following model to explain (1) the occurrence of volcanism off the hotspot track, (2) the coupling of Madeira and Desertas volcanism, and (3) the concept of distinct regions of melt extraction whilst maintaining geochemical continuity.

Island spacing of hotspot systems can be controlled by lithosphere flexure due to the load of volcanic shields (Ten Brink 1991). At the transition between flexural depression and bulge, where horizontal flexural stresses are approximately zero, magma flow to the surface may be facilitated, forming a new volcano. For a steady source of melt underneath a moving lithospheric plate, this process produces a chain of discrete volcanoes along a single or dual line (Hieronymus and Bercovici 1999). In contrast, the Madeira hotspot track is ascribed to a weak, pulsating plume (Geldmacher et al. 2000), the shape and flow of which may be influenced by mantle convection. It is conceivable that such a pulsating plume becomes irregularly shaped, causing lateral variations of the melting region. Combined with the flexure model of Ten Brink (1991), this effect could result in a disperse volcano pattern, rather than a line. Although data are lacking, a lithosphere flexure beneath the Madeira Archipelago is likely when compared to the analogous situation of the western Canary Islands (Collier and Watts 2001). We thus presume that the Desertas ridge is located at a lithospheric bend caused by the Madeira and Porto Santo loads, a location with a stress field facilitating ascent of magmas through the lithosphere (Fig. 8). Lateral variations of the melting region, combined with slow plate motion and flexural stress, could have initiated the Desertas volcanism off the hotspot track and caused the shift of activity between Madeira and the Desertas (Fig. 8). This model is in accordance with the geochemical continuity of the Madeira/Desertas complex over time (Geldmacher and Hoernle 2000), which requires a common magma source for both.

Conclusions

The results presented in this paper show that thermobarometric data not only provide information about the depths of magma fractionation and stagnation, but additionally allow inferences on relations between adjacent volcanic systems to be made. Fluid inclusion data as well as mineral-melt barometry indicate systematic differences as well as some similarities between the magma plumbing systems beneath the rift zones of São Lourenço/Madeira and the adjacent Desertas Islands. For both systems, levels of magma fractionation and stagnation were identified within both the uppermost mantle and the crust. São Lourenço samples of Early and Late Madeira rift phases indicate similar levels of magma stagnation within the crust which differ from those beneath the Desertas. This observation suggests that there is no common shallow magma reservoir feeding both the Madeira and the Desertas rifts. A deeper interconnection of the two rift systems within the uppermost mantle or the lower crust by lateral magma transport appears unlikely. We propose that Madeira and the Desertas represent two separate volcano systems, rather than a single volcanic complex with two rift arms. Distinctive magma pathways down to at least 35 km depth imply that both volcanoes root in distinct regions of partial melting within the Madeira plume. The shift of volcanic activity between Madeira and the Desertas may be a result of lateral variations of the melting region in an irregularly shaped

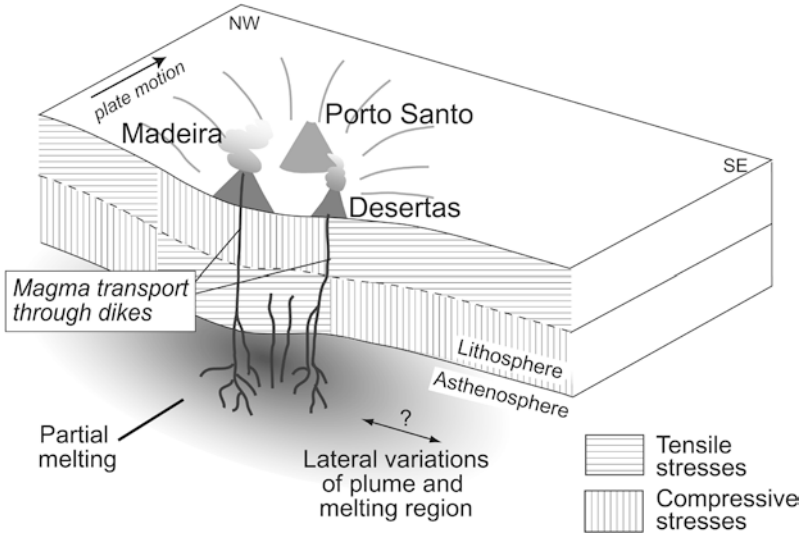

Fig. 8 Schematic section through the lithosphere beneath Madeira perpendicular to plate motion, illustrating the influence of lithosphere flexure on magma ascent (modified after Hieronymus and Bercovici 1999). Hypothetical lithosphere bending due to the load of Madeira and Porto Santo is strongly exaggerated. At the transition between flexural depression and flexural bulge, horizontal stresses are approximately zero, facilitating rise of magma through dikes up to the surface aside the hotspot axis and causing the Desertas volcanism

plume, combined with flexural stresses within the lithosphere due to the loads of Madeira and Porto Santo. This model could explain the shift of volcanic activity between Madeira and the Desertas Islands, and possibly of other hotspot volcanoes as well.

Acknowledgements We thank directors Costa Neves and Susana Fontinha and the staff of the Parque Natural da Madeira for their logistical support during our field studies on São Lourenço and the Desertas Islands. Without their help the study of the islands would not have been possible. Bärbel Kleinefeld is acknowledged for help during microthermometric analysis and for providing Raman measurements. Especial thanks go to Andreas Kronz, Heidi Höfer and Peter Appel for assisting with the EMP measurements. The paper benefited from discussions with Colin Devey, and early versions of the manuscript improved through the critical comments of Kaj Hoernle and the constructive reviews of Thor Hansteen and Tom Andersen. The research was supported by the Deutsche Forschungsgemeinschaft (DFG grant KL1313/2-1).

Appendix

Xenolith petrography

DES4

Spinel wehrlite consisting to about 80% of early-formed olivine up to 3 mm with some kink bands, and 20% of interstitial clinopyroxene with abundant melt inclusions. Cpx is associated with late-formed and smaller, euhedral to subhedral olivines (<0.5 mm) and small spinels (<250 μm). Fine-grained spinels (about 20 μm) occur throughout the xenolith. Low intracrystalline deformation and the occurrence of interstitial clinopyroxene with olivine inclusions is evidence for a cumulate origin of the xenolith.

DGR132

Spinel dunite with coarse-grained olivine up to 8 mm in size showing abundant kink bands, melt and fluid inclusions, and euhedral to subrounded spinel up to 0.6 mm in size. Basaltic matrix of fine-grained clinopyroxene, olivine and plagioclase locally occurs in cracks and pockets and is interpreted as host melt which penetrated along grain boundaries and cracks. The dunite xenoliths are interpreted as cumulates.

M51/1-437DR-1

Harzburgite from the submarine Funchal ridge with abundant fluid inclusions. Olivine porphyroclasts (about 80%) from 1 to 6 mm in size show curvilinear grain boundaries and abundant kink bands. Orthopyroxenes porphyroclasts (20%) with clinopyroxene exsolution lamellae show embayments at the xenolith surface, demonstrating that they have reacted with the surrounding melt. No oxide minerals were found. Because of the deformation indicated by kink bands and the resorbed pyroxenes rims, the xenolith is interpreted to represent a fragment of the refractory mantle beneath Madeira.

References

Andersen T, Neuman E-R (2001) Fluid inclusions in mantle xenoliths. Lithos 55:301–320 DOI 10.1016/S0024-4937(00)00049-9

Andersen T, O'Reilly SY, Griffin WL (1984) The trapped fluid phase in upper mantle xenoliths from Victoria, Australia: implications for mantle metasomatism. Contrib Mineral Petrol 88:72–85

Angus S, Armstrong B, de Reuck KM, Altunin VV, Gadetskii OG, Chapela GA, Rowlinson JS (1976) Carbon dioxide (International tables of fluid state, vol 3). Pergamon Press, Oxford

Bakker RJ, Jansen JBH (1991) Experimental post-entrapment water loss from synthetic CO_2-H_2O inclusions in natural quartz. Geochim Cosmochim Acta 55:2215–2230 DOI 10.1016/0016-7037(91)90098-P

Banda E, Dañobeitia JJ, Surinach E, Ansorge J (1981) Features of crustal structure under the Canary Islands. Earth Planet Sci Lett 55:11–24

Belkin HE, De Vivo B (1993) Fluid inclusion studies of ejected nodules from plinian eruptions of Mt. Somma-Vesuvius. J Volcanol Geotherm Res 58:89–100 DOI 10.1016/0377-0273(93)90103-X

Brown PE (1989) FLINCOR: a fluid inclusion data reduction and exploration program. In: Program Abstr Vol 2nd Biennal Pan-Am Conf Fluid Inclusions, 4–7 January 1989, Virginia Polytechnic Institute, State University, Blacksburg, VA, pp 14

Carracedo JC (1994) The Canary Islands: an example of structural control on the growth of large ocean-island volcanoes. J Volcanol Geotherm Res 60:225–241 DOI 10.1016/0377-0273(94)90053-1

Clague DA (1987) Hawaiian xenolith populations, magma supply rates, and development of magma chambers. Bull Volcanol 49:577–587

Collier JS, Watts AB (2001) Lithospheric response to volcanic loading by the Canary Islands: constraints from seismic reflection data in their flexural moat. Geophys J Int 147:660–676 DOI 10.1046/j.0956-540x.2001.01506.x

Delaney PT, Fiske RS, Miklius A, Okamura AT, Sako K (1990) Deep magma body beneath the summit and rift zones of Kilauea Volcano, Hawaii. Science 247:1311–1316

De Vivo B, Frezzotti ML, Lima A, Trigila R (1988) Spinel lherzolite nodules from Oahu island (Hawaii): a fluid inclusion study. Bull Minéral 111:307–319

Dietrich JH (1988) Growth and persistence of Hawaiian volcanic rift zones. J Geophys Res 93:4258–4270

Dixon JE, Clague DA, Wallace P, Poreda R (1997) Volatiles in alkalic basalts from the North Arch volcanic field, Hawaii: extensive degassing of deep submarine-erupted alkalic series lavas. J Petrol 38:911–939

Duffield WA, Christiansen RL, Koyanagi RY, Peterson D W (1982) Storage, migration and eruption of magma at Kilauea Volcano, Hawaii, 1971–1972. J Volcanol Geotherm Res 13:273–307

Duke JM (1976) Distribution of the period transition elements among olivine, calcic clinopyroxene and mafic silicate liquid: experimental results. J Petrol 17:499–521

Eaton JP, Murata KJ (1960) How volcanoes grow. Science 132:925–938

Ford CE, Russell DG, Craven JA, Fisk MR (1983) Olivine-liquid equilibria: temperature, pressure and composition dependence of the crystal/liquid cation partition coefficients for Mg, Fe2+, Ca and Mn. J Petrol 24:256–265

Frezotti ML, Andersen T, Neumann E-R, Simonsen SL (2002) Carbonatite melt-CO_2 fluid inclusions in mantle xenoliths from Tenerife, Canary Islands: a story of trapping, immiscibility and fluid-rock interaction in the upper mantle. Lithos 64:77–96

Geldmacher J, Hoernle KA (2000) The 72 Ma geochemical evolution of the Madeira hotspot (eastern North Atlantic): recycling of Paleozoic (500 Ma) oceanic lithosphere. Earth Planet Sci Lett 183:73–92 DOI 10.1016/S0012-821X(00)00266-1

Geldmacher J, Bogaard P v d, Hoernle KA, Schmincke HU (2000) The $^{40}Ar/^{39}Ar$ age dating of the Madeira Archipelago and hotspot track (eastern North Atlantic). G3 Geochem Geophys Geosys 1:1999GC000018

Gudmundsson A (1995) Infrastructure and mechanism of volcanic systems in Iceland. J Volcanol Geotherm Res 64:1–22 DOI 10.1016/0377-0273(95)92782-Q

Hansteen TH, Klügel A, Schmincke HU (1998) Multi-stage magma ascent beneath the Canary Islands: evidence from fluid inclusions. Contrib Mineral Petrol 132:48–64 DOI 10.1007/s004100050404

Hieronymus CF, Bercovici D (1999) Discrete alternating hotspot islands formed by interaction of magma transport and lithospheric flexure. Nature 397:604–607 DOI 10.1038/17584

Hoernle KA, Shipboard Scientific Party (2001) Meteor-Berichte, Cruise 51, Leg 1. In: Hemleben C, Hoernle KA, Jørgensen BB, Roether W (eds) Ostatlantik-Mittelmeer-Schwarzes Meer, Cruise No. 51, 12 September-28 Dezember 2001. Universität Hamburg, Meteor-Berichte 03-1

Kerrick DM, Jacobs GK (1981) A modified Redlich-Kwong equation for H_2O, CO_2 and H_2O-CO_2 mixtures at elevated temperatures and pressures. Am J Sci 281:735–767

Klügel A, Hoernle KA, Schmincke H-U, White JDL (2000) The chemically zoned 1949 eruption on La Palma (Canary Islands): petrologic evolution and magma supply dynamics of a rift-zone eruption. J Geophys Res 105:5997–6016

Le Maitre RW, Bateman P, Dudek A, Keller J, Lameyre J, Le Bas MJ, Sabine PA, Schmid R, Sorensen H, Streckeisen A, Wooley AR, Zanettin B (1989) A classification of igneous rocks and glossary of terms—recommendations of the International Union of Geological Sciences Subcommission on the Systematics of Igneous Rocks. Blackwell, Oxford, pp 193

MacDonald GA (1968) Composition and origin of Hawaiian lavas. In: Coats RR, Hay RL, Andersen CA (eds) Studies in volcanology: a memoir in honour of Howel Williams. Geol Soc Am Mem 116:477–522

Munha J, Palacios T, MacRae ND, Mata J (1990) Petrology of ultramafic xenoliths from Madeira island. Geol Mag 127:543–566

Pitman W, Talwani M (1972) Sea floor spreading in the north Atlantic. Geol Soc Am Bull 83(3):619–646

Putirka K (1997) Magma transport at Hawaii: Inferences based on igneous thermobarometry. Geology 25:69–72 DOI 10.1130/0091-7613(1997)025<0069:MTAHIB>2.3.CO;2

Putirka K, Johnson M, Kinzler R, Longhi J, Walker D (1996) Thermobarometry of mafic igneous rocks based on clinopyroxene-liquid equilibria, 0–30 kbar. Contrib Mineral Petrol 123:92–108 DOI 10.1007/s004100050145

Roedder E (1965) Liquid CO_2 inlcusions in olivine-bearing nodules and phenocrysts from basalts. Am Mineral 50:1746–1782

Roedder E (1983) Geobarometry of ultramafic xenoliths from Loihi Seamount, Hawaii, on the basis of CO_2 inclusions in olivine. Earth Planet Sci Lett 66:369–379

Roedder E (1984) Fluid inclusions. In: Ribbe PH (ed) Reviews in Mineralogy 12. Mineral Soc Am, Washington, DC

Roedder E, Bodnar RJ (1980) Geologic pressure determinations from fluid inclusion studies. Annu Rev Earth Planet Sci 8:263–301

Roeder PL, Emslie RF (1970) Olivine-liquid equilibrium. Contrib Mineral Petrol 29:275–289

Roeser HA (1982) Magnetic anomalies in the magnetic quiet zone off Morocco. In: Rad UV, Hinz K, Sarntheim M, Seibold E (eds) Geology of the northwest African continental margin. Springer, Berlin Heidelberg New York, pp 61–68

Ryan MP (1988) The mechanics and three-dimensional internal structure of active magmatic systems: Kilauea volcano, Hawaii. J Geophys Res 93:4213–4248

Sachs PM, Hansteen TH (2000) Pleistocene underplating and metasomatism of the lower continental crust: a xenolith study. J Petrol 41:331–356

Smith WHF, Sandwell DT (1997) Global seafloor topography from satellite altimetry and ship depth soundings. Science 277:1956–1962

Szábo CS, Bodnar RJ (1996) Changing magma ascent rates in the Nógrád-Gömör volcanic field Northern Hungary/Southern Slovakia: evidence from CO_2-rich fluid inclusions in metasomized upper mantle xenoliths. Petrology 4:240–249

Ten Brink U (1991) Volcano spacing and plate rigidity. Geology 19:397–400

Tilling RI, Dvorak JJ (1993) Anatomy of a basaltic volcano. Nature 363:125–133

Walker GPL (1999) Volcanic rift zones and their intrusion swarms. J Volcanol Geotherm Res 94:21–34 DOI 10.1016/S0377-0273(99)00096-7